Conference Proceedings

Solar World Congress 2015
Daegu, Korea, 08 – 12 November 2015

Analysis of a silica glass based high temperature thermal energy storage unit for concentrated solar power applications

Bruno Cárdenas[1], Noel León[1], Martin H. Bremer[1] and John Pye[2]

[1] Tecnologico de Monterrey, Campus Monterrey, Monterrey (México)

[2] Australian National University, Canberra (Australia)

Abstract

The design of a directly-charged high temperature thermal energy storage (TES) unit based on molten silica-glass is presented. The 126 kWh_{th} thermal storage unit developed is aimed to operate within a solar-driven domestic scale power generation system.

The paper discusses the proposed design for the unit as well as the restrictions set by the power generation system's requirements. The transient mathematical model used to analyze the behavior and performance of the thermal energy storage unit during the different stages of the intended work cycle is thoroughly explained. An important feature of the mathematical model is that the performance of the unit is not only evaluated from an energy viewpoint, but an in-depth exergy analysis has been additionally carried out.

The results obtained through the model are exhaustively analyzed; special focus has been given to the assessment of the performance of the storage unit to guarantee that the operational requirements of the power generation system are met. The overall performance of the TES unit is satisfactory; the unit is capable of supplying the required 4 kW_{th} output throughout the 16-hour discharge while it reaches its fully charged state during the subsequent 8-hour recharge. The proposed designed for the TES unit exhibits a round trip exergy-efficiency of 59%.

Keywords: *Solar thermal energy storage, molten silica glass, high temperature heat storage, thermal storage exergy analysis*

1. Introduction

One of the major difficulties solar based electric power generation systems face is the intermittent nature of the solar resource; therefore effective methods for storing the excess thermal energy collected during periods of high solar irradiation or periods of low energy demand are needed (Hasnain,1998).

Thermal energy can be stored in three different ways: as sensible heat, as latent heat or as chemical potential through reversible chemical reactions. (Sharma et al. 2009). Latent heat storage (LHS) offer a number of benefits over sensible heat storage systems (SHS) such as higher energy densities and a nearly isothermal energy output at the phase change temperature (Zalba et al. 2003, Farid et al. 2004, Kenisarin, 2010).

An enormous amount of research has been devoted to the development of LHS systems, which are deemed as a very promising technology; however, their widespread utilization has been slowed down by the low thermal conductivity of phase change materials (PCM) and other drawbacks related to their use. (Liu et al. 2012, Cárdenas and León, 2013. Liu et al. 2015). Nowadays, large scale concentrated solar power (CSP) plants still use sensible heat materials such as rocks, synthetic oils and molten salts. A more thorough description of the state of the art of thermal energy storage for power generation can be found in the literature (Gil et al. 2010, Medrano et al. 2010, Ushak, 2015, Steinmann, 2015),

doi:10.18086/swc.2015.02.02 Available at http://proceedings.ises.org

It has been broadly demonstrated that LHS has many advantages over SHS; however, there are materials whose potential as sensible storage medium has not been carefully considered yet, despite possessing outstanding properties, as is the case of soda-lime silica glass, which has high specific heat capacity, it is remarkably cheap and it is neither flammable, corrosive nor toxic.

The present research work focuses on the design and modeling of a soda-lime silica glass based high temperature thermal energy storage (TES) unit with the objective of laying the groundwork on the utilization of recycled soda-lime silica glass as a thermal energy storade medium. The unit will work in a novel solar driven micro-CHP (combined heating and power) system; however, it is thought that the concept could be scaled-up for larger CSP applications.

2. Operation within the micro-CHP system

The TES unit will operate within a solar-driven domestic distributed power generation system in which solar radiation is captured through a 30 m^2 Fresnel lens (Ramirez, 2015). Considering the solar irradiation in Monterrey, Mexico, the Fresnel Lens supplies an average power of 18.75 kW_{th} during daytime (idealized as an 8-hour period). The concentration spot of the lens strikes directly onto the reception surface of the TES unit, whose interior is filled with soda-lime silica glass (recycled from windows and bottles) that acts as the heat storage medium. As the solar radiation enters the TES unit the temperature of the storage medium increases until reaching approximately 1000°C; storing thus the incoming solar energy in the form of heat. The TES unit is connected through a heat exchanger to a 1 kW_e Stirling engine with an estimated efficiency of 30 %, which will generate electric power continuously throughout the day.

The TES unit will operate in a temperature range from 500°C to 1000°C; below 500°C the TES unit is not able to maintain the Stirling engine operating. The cyclic operation of the unit comprises two stages: an 8-hour charge (storage) period and a 16-hour discharge period . In addition to that, there is an initial charging step (not part of the cycle) in which the TES unit is brought from ambient temperature to its operating temperature of 1000°C at the heat extraction surface.

During the 16-hour (corresponding to the remaining 2/3 of the day) discharge step, the TES unit has to deliver 4 kW_{th} (defined based on the Stirling efficiency and heat exchanger losses) with no solar input. The temperature of the heat extraction surface must remain above 500 °C during the whole period. Then follows the 8-hour recharge stage in which the TES receives solar radiation once again but still maintains the 4 kW_{th} output. At the end of the recharge period, the temperature of the heat extraction surface must have reached 1000°C, so that the TES unit is fully charged and is able to undergo the subsequent 16-hour discharge period, thus maintaining a cyclic operation.

3. Concept developed for the TES unit

The TES unit proposed, shown in Figure 1, consists of a prismatic refractory concrete container whose interior is divided into smaller cavities by several equidistant vertical graphite slabs (walls), between which the approximate 82 L of glass are distributed. Two grooved rectangular graphite plaques keep the walls in vertical position and evenly spaced inside the container. The TES unit has a storage capacity of 126.3 kWh_{th} when fully charged (i.e. when the heat extraction surface is at 1000° C). The outer dimensions of the unit including insulation are: a length of 143.2 cm, a depth of 90.5 cm and a total height of 68.4 cm.

The concentrated solar radiation coming from the lens enters the TES unit through its top side (due to a system requirement) and is conducted inwards by means of the vertical walls. The walls are designed to enhance the internal heat transfer, as the soda-lime silica glass to be used has a very low thermal conductivity; facilitating thus the charge and discharge of the TES unit and helping to achieve a uniform temperature distribution throughout its interior.

The heat extraction is carried out by means of a heat transfer fluid (HTF) in contact with the bottommost graphite surface; the design of the heat exchanger design is out of the scope of the present paper and will not be discussed. In addition to the use of a heat transfer enhancement method (the vertical graphite walls), the height of the TES unit was kept to a minimum for allowing the heat stored in the upper portions of glass to

reach the discharge area rapidly and impeding it from prematurely reaching the 500°C limit.

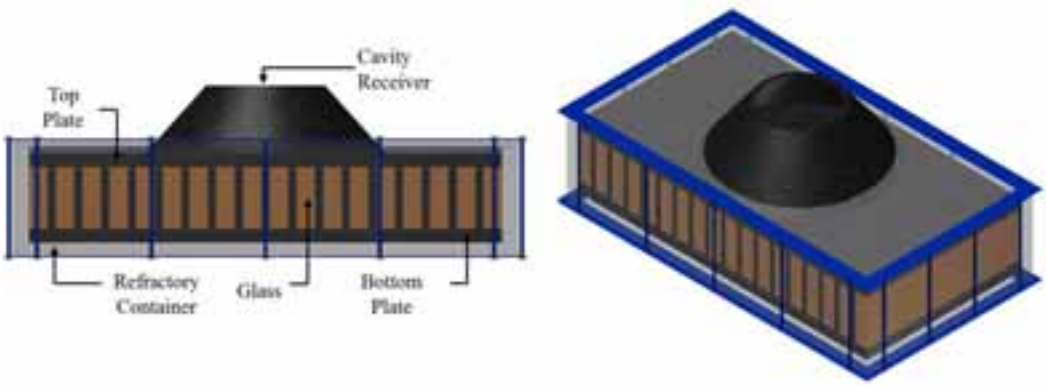

Figure 1. Views of the core of the proposed TES unit design

The cavity receiver was designed trying to emulate a blackbody, although further work is intended to refine the design. The incident solar rays are reflected many times on the interior before finally escaping from the aperture; with each reflection a fraction of the energy, is absorbed and after many reflections, the incoming radiation is mostly absorbed. The temperature of the material will increase, it will start to radiate heat and the same effect will occur; the cavity wall will absorb its own radiation and heat losses will be minimized. A radiation shape factor $F_{1\text{-}2}$ of 0.205 was achieved, which means that 20.5% of the heat that the bottom surface irradiates escapes through the aperture while 79.5 % is re-absorbed by the lateral wall of the cavity.

4. Mathematical modeling of the performance of the TES unit

4.1 Transient mathematical model developed

A transient mathematical model was developed for analyzing the thermal behavior of the TES unit throughout the cyclic operation. The model is primarily based on equations (Eq.1) and (Eq.2), the former being the one-dimensional heat conduction equation and the latter being the first law of thermodynamics for an incompressible material:

$$Q = (k \cdot A \cdot \Delta T \cdot \Delta t)/\Delta x \quad \text{(Eq.1)}$$

$$Q = m \cdot C_p \cdot \Delta T \quad \text{(Eq.2)}$$

The model originates with two main assumptions; the first one is that within a component there are no temperature gradients, meaning that the temperature is uniform over the cross-sectional area of each element. The second one is that there is no convection in the molten glass due to its elevated viscosity, which is 104 Pa·s at the flow point (920 °C) for the average composition of soda–lime silica glass. (Shand, 1958); thus, all the internal heat transfer during the complete work cycle of the TES unit is assumed to be due only to conduction.

To perform the calculations each component of the geometry of interest is divided into elements. Thereafter, an energy balance is made for each element stating that the difference between the energy entering and the energy leaving the element over a certain time-step is equal to the energy that is stored by the element.

The energy balance is performed for every element over n time-steps until a certain time or condition such as a final temperature is reached. During a given time-step a certain amount of heat is received by an element n at a temperature *T*. During the same time-step some energy leaves the element *n*, which is still at the same temperature *T*; a part of the energy leaving the element goes into the next element *n+1* while another part of it is lost to the ambient, depending the case. The difference between the energy that the element n received minus the energy conducted from the element n to the element *n+1* and the lost heat, is the energy stored by the element *n* during that particular time-step.

The energy stored by the element causes an increase in its temperature, given by Eq.2; this increase in temperature entails a change in the specific heat capacity and thermal conductivity of the material. It is

important to mention that in order for the model to have numerical stability and accurately simulate the real heat transfer phenomena a previous study (sensibility analysis) for determining the maximum time step permissible, which is a function of mesh size and temperature differences, must be carried out.

The interactions between elements are explained graphically in Figure 2. A power input of 18.75 kW_{th} (average power supplied by the Fresnel lens) is applied to the top-most surface of the top graphite plate, which conducts energy to both, glass and graphite elements in contact with its lower surface.

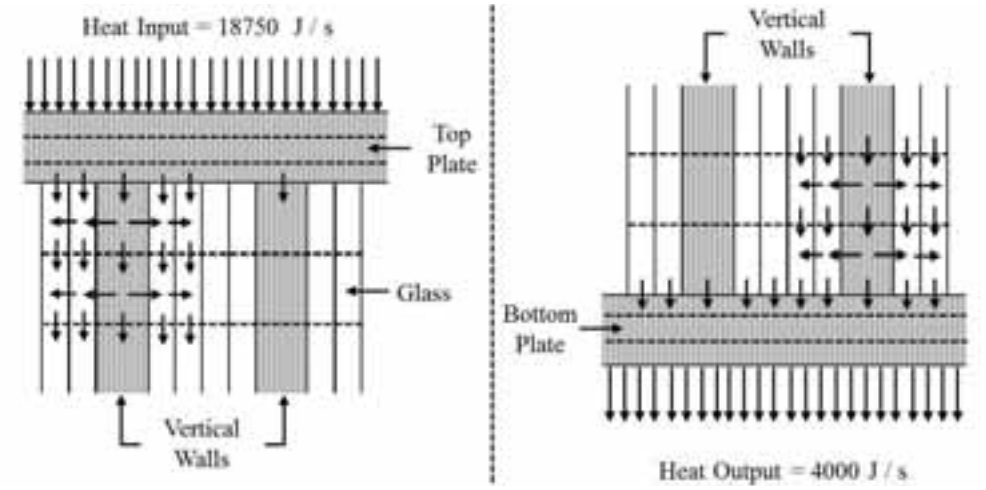

Figure 2. Thermal interactions between elements of the geometry defined for the model

The behavior of every graphite wall and the glass in the cavity next to it is assumed to be the same for every wall-cavity set; therefore only one graphite wall and the glass at one if its sides are calculated. The elements of the graphite wall conduct heat downwards to the next element of the wall and sideways to the glass next to them. The first element of glass, in a similar fashion, conducts heat to the glass element below it and to the glass element on its side; finally, the second glass element conducts heat exclusively downwards into the glass element below it. The other half of the glass in the cavity is assumed to be heated by the contiguous graphite wall; i.e. each graphite wall only interacts with half of the glass on the cavity next to it.

The bottom graphite plate receives heat from the glass and graphite elements above it, as shown in Figure 4. Except for the initial charge period, a load of 4 kW_{th} is permanently applied to its bottom-most surface to simulate the energy discharge.

The model does not calculate the temperature increase of the graphite frustum. It is assumed that the piece is able to absorb all the incident radiation that is reflected by itself; therefore, an absorptivity of 1.0 was employed for the graphite. The radiative losses were calculated based on the area of the bottom surface of the frustum and the calculated shape factor of 0.205; as aforementioned, only 20.5% of what the surface is emitting is actually lost to the surroundings.

Polynomial equations were created for the temperature dependent properties of the main materials, i.e. graphite and an average composition of soda-lime silica glass. The equations created follow the general form shown in Eq.3 and represent the average of the experimental data presented by several authors. Table 1 provides the coefficients for the calculation of the specific heat capacity (C_p) and thermal conductivity (k) of both materials.

$$C_p, k = AT^5 + BT^4 + CT^3 + DT^2 + ET + F \quad \text{(Eq.3)}$$

An important aspect of the mathematical model is the exergy analysis of the TES unit. In addition to calculating via the energy balance the energy stored by an element *n* during every time-step, the total energy accumulated by each element is also accounted for. This makes possible calculating the total exergy stored by the element through the exergy equation for an incompressible mass (Eq.4), and consequently, the exergy destroyed as well as the exergy-based efficiency of the TES unit.

$$X = (U - U_0) - T_0(S - S_0) \quad \text{(Eq.4)}$$

Tab.1: Coefficients for the calculation of the temperature dependent properties of soda-lime silica glass and graphite

Property	Coefficients		Source(s)
Glass specific heat capacity (J/g·K)	A= 9.474×10^{-15} B= -3.923×10^{-11} C= 6.221×10^{-8}	D= -4.746×10^{-5} E= 1.814×10^{-2} F= -1.833	Shand, 1958 Stebbins et al, 1984 Richet, 1987 Huang and Gupta, 1992
Glass thermal conductivity (W/m·K)	A= -1.413×10^{-14} B= 6.083×10^{-11} C= -3.120×10^{-8}	D= -2.853×10^{-5} E= 2.512×10^{-2} F= -3.668	Shand, 1958
Graphite specific heat capacity (J/g·K)	A= -4.257×10^{-16} B= 1.093×10^{-12} C= 5.638×10^{-10}	D= -4.514×10^{-6} E= 5.645×10^{-3} F= -6.034×10^{-1}	Butland and Maddison, 1974 Nihira and Iwata, 2003
Graphite thermal conductivity (W/m·K)	A= -2.370×10^{-14} B= 1.393×10^{-10} C= -3.373×10^{-7}	D= 4.429×10^{-4} E= -3.611×10^{-1} F= 209.893	Rasor and McClelland, 1960 Wagner and Dauelsberg, 1967 Bapat, 1973 Bapat and Nickel, 1973 Madelung and White, 1991

In the model, an exergy balance (Eq.5) is performed every time-step for each of the elements defined to obtain the exergy destruction at every element of the system. One of the difficulties the exergy analysis presents is quantifying the exergy content of the incident solar radiation, since the balance requires an exergy input for the calculation. Eq.6 is used as the exergy input for the balance (Petela, 2003) in which i is the amount of solar radiation, α is the absorptance of the material, and T_{sun} is considered as 5778 K.

$$X_{in} - X_{out} - X_{dest} = \Delta X_{system} \quad \text{(Eq.5)}$$

$$X_{Sun} = i\left[1 + \frac{1}{3}\left(\frac{T_0}{T_{sun}}\right)^4 - \frac{4}{3}\left(\frac{T_0}{T_{sun}}\right)\right]\alpha \quad \text{(Eq.6)}$$

The exergy transfer (X_{in}, X_{out}) comes from the heat transfer (Q) from an element at a certain temperature T to another element, for the case of conducted heat it may be accounted for as follows:

$$X_{heat} = (1 - T_0/T) \cdot Q \quad \text{(Eq.7)}$$

Evaluating a system exclusively through an energy-based efficiency could be misleading; because, even though most of the incoming energy is conserved or recovered, it will be degraded by all the internal heat transfer that occurs during the storage process causing the loss of some potential for performing work.

A notable aspect of the model developed is that it can be used for a different storage material other than soda-lime silica glass as long as the consideration of no convection is not overlooked. If it is desired to calculate the performance of a TES unit with a different storage material that undergoes a phase transition from solid to liquid, or is liquid the whole time, it is very important to evaluate if due to its viscosity and the size of the cavities in which it is contained the assumption of no convection is valid. If the storage medium is a solid material, either crystalline or amorphous, and stays solid throughout the work cycle, the model is applicable right away.

4.2 Analysis of the behavior and performance of the TES unit

Not all of the temperature profiles calculated through the mathematical model are displayed in the following Figures for the sake of an easier understanding; however, the profiles presented depict accurately the overall behavior of the TES unit. Figure 3 shows the geometric location within the unit of each of the temperature profiles shown further on in the graphs, i.e. where the temperatures are “measured”.

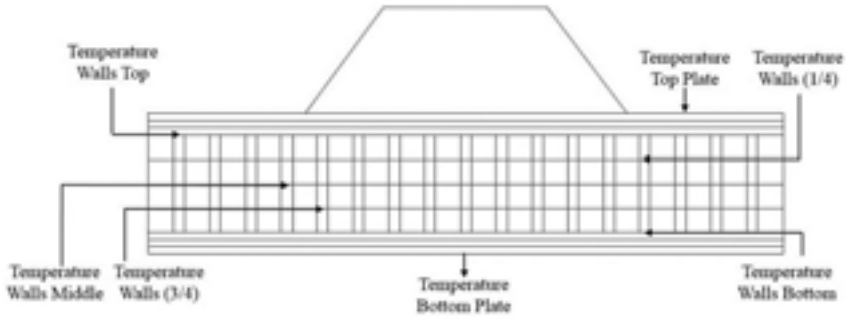

Figure 3. Geometric locations within the TES unit of some representative temperature profiles

Figure 4 shows the temperature profiles of some elements during the initial charge period, in which the 4 kW output is not present. As expected, the temperature of the first element of the top plate (where radiation strikes) is the first to increase followed by the temperatures of the rest of the elements of the different components. The temperatures, except for a short period at the beginning of the heating, increase at a very constant rate; the maximum difference between the temperature of the top plate and the temperature of the bottom plate recorded during the heating process is 87.8°C while an average difference of 76.7°C was observed throughout the heating process.

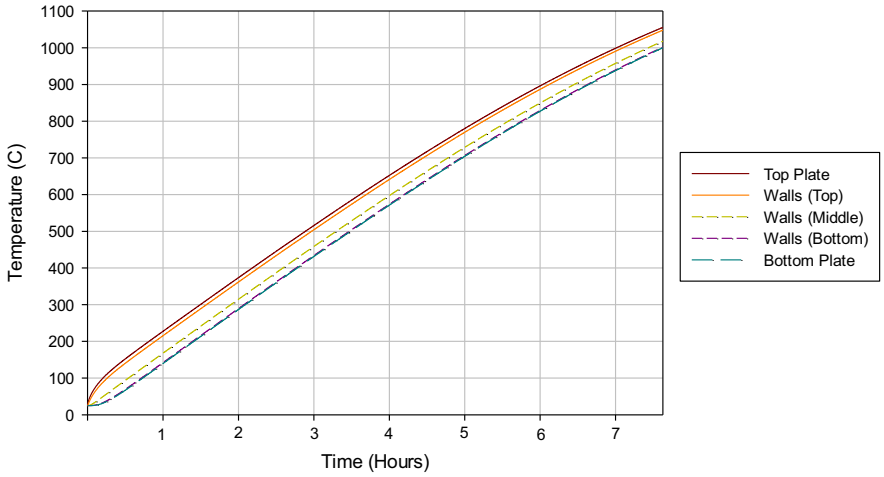

Figure 4. Representative temperature profiles during the initial charge period

The TES unit reaches its goal temperature of 1000°C in the lower surface of the bottom plate in approximately 7 hours and 38 minutes. From a micro-CHP system point of view, this is quite convenient since the TES unit could be heated up from ambient temperature to its operating temperature in 1-day time with the Fresnel lens and no external aid.

It is noteworthy that the temperature profiles of the glass elements are not included in Figure 4; the reason for this is that throughout the entire heating process the profiles of the two glass elements adjacent to each of the 30 vertical graphite wall elements maintain a very close temperature to that of their respective wall element. During the complete heating process, the difference between the temperature of the glass elements and the graphite wall element never surpassed 4°C, this rather small temperature difference suggests that the vertical graphite walls are well spaced inside the refractory container and that they are indeed facilitating the distribution of the thermal energy in the interior of the TES unit.

Figure 5 shows the temperature profiles of some representative elements of the TES unit during the discharge (or cooling) period obtained through the mathematical model. The state of the elements after the last time-step of the initial charge period is used as the starting point for the discharge stage. A load of 4 kW_{th} is applied to the bottom-most element of the bottom plate and both, the heat input and radiation losses, are set to zero; assuming that during the discharge period the cavity could be covered with insulation since there need not be an aperture for the concentrated beam from the lens.

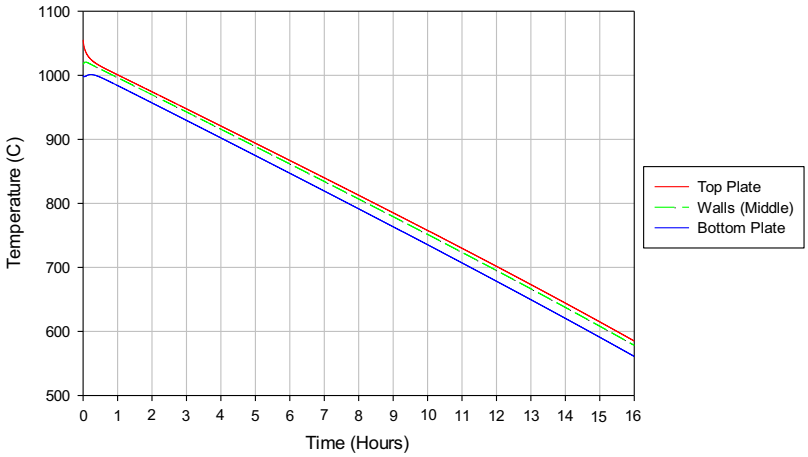

Figure 5. Representative temperature profiles during the 16-hour discharge period

As can be seen, the TES unit is capable of supplying the constant 4 kWth during the required 16-hour period, at the end of which the temperature of the bottom plate is 561°C while the temperature of the top plate is 585°C, a difference of just 24°C. The reduced height of the unit helped to minimize the temperature difference between the top and bottom plates; having such a small temperature difference at the end of the discharge period indicates a very thorough discharge of the TES unit.

Similarly to the initial charge period, the temperatures of the two glass elements adjacent to each of the 30 vertical graphite wall elements remain very similar to the temperature of their respective wall element throughout the complete discharge period. The difference between the temperature of the glass elements and the elements of the vertical wall never exceeds 2.5°C.

Figure 6 shows the temperature profiles of some representative elements during the recharge (storage) period, in which the heat input from the Fresnel is available once again but the 4 kWth output is still supplied. The last time step of the discharge process is used as the starting point for the 8-hour recharge stage. During this period, the lower surface of the bottom plate must reach 1000 °C so the TES unit is able to undergo the following 16-hour discharge period, thus maintaining a cyclic operation.

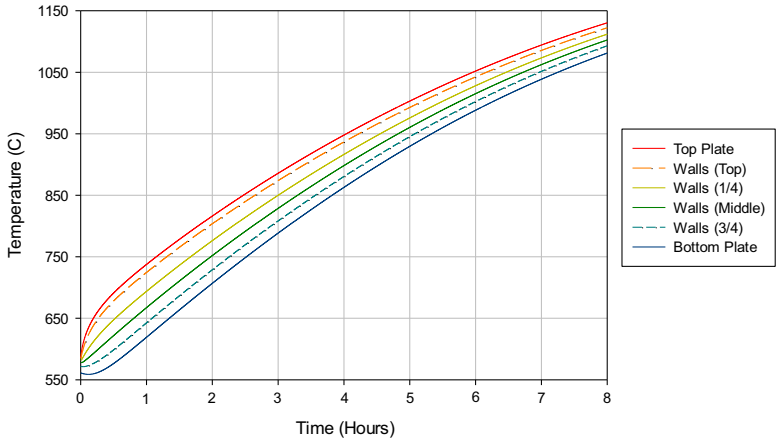

Figure 6. Representative temperature profiles during the 8-hour recharge period

The temperature profiles spread at the beginning of the heating; slightly before the first hour of heating the maximum temperature difference between the top and bottom plates of 118.8°C is reached; after this point the temperature difference between elements decreases with time. The average temperature difference between the topmost and bottommost temperature profiles throughout the complete period is 84.1°C. The temperature of the glass elements is, like in the initial charge and discharge periods, still very close to the temperature of their respective wall elements.

It may be noted that higher temperatures than those used at the starting point of the discharge are reached.

This overshoot may be eliminated, for instance, by defocusing the Fresnel lens of the micro-CHP system; however, it is not necessarily an issue. Reaching higher temperatures than necessary at the end of the recharge means that there is some tolerance in the system that would allow the TES to be fully charged in days with less-than-average conditions when the Fresnel is not capable of supplying the average 18.75 kW_{th} considered in the model. The complete work cycle of the TES unit is shown in Figure 7; the highest and lowest temperature profiles within the unit are displayed in red and blue, respectively. All the other profiles comprised between them are not presented for an easier understanding.

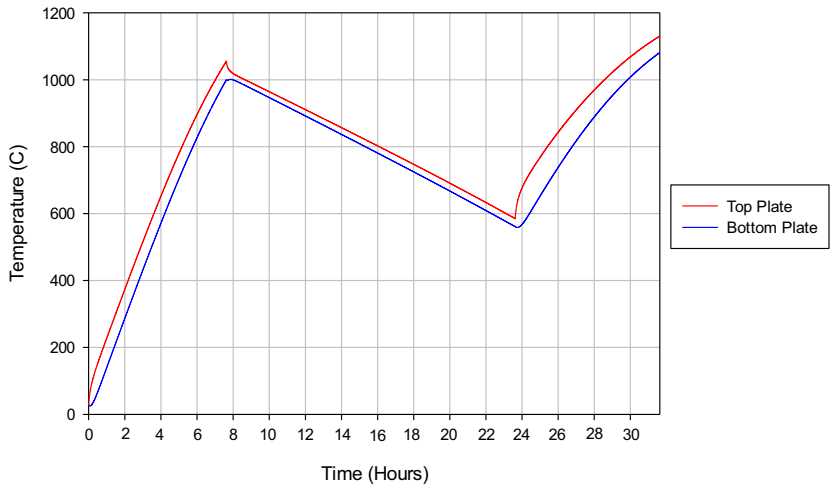

Figure 7. Highest and lowest temperature profiles throughout the complete work cycle

The change in the energy stored by the TES unit throughout the complete work cycle and its distribution in each of the components is shown in Figure 8. At the end of the initial charge period the TES unit has 454.87 MJ (126.35 kWh_{th}) of thermal energy stored, of which 51% is stored in the glass, 19.2 % in the graphite walls, 15.4 % in the top plate and 14.4 % in the bottom plate.

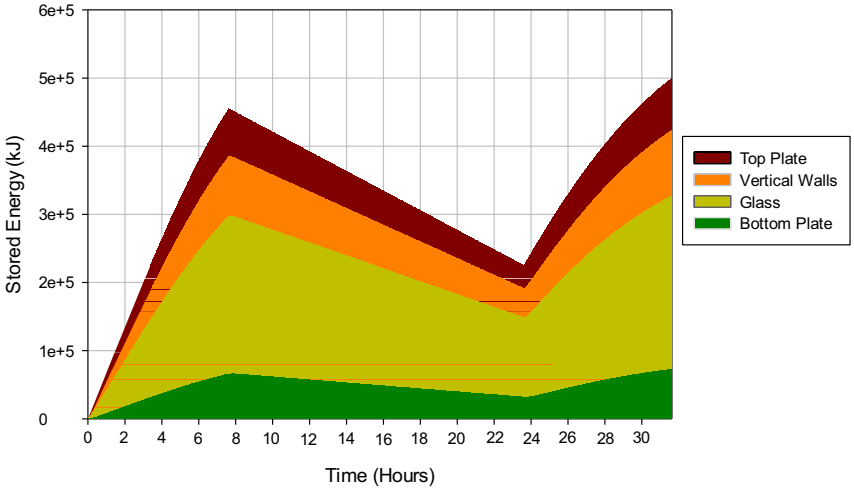

Figure 8. Energy stored in the TES unit throughout the complete work cycle

At the end of the discharge the TES unit is practically out of usable energy, only 0.964 MJ (0.26 kWh_{th}) are left in the unit, meaning that the concept developed allows a very thorough heat extraction. It is important to emphasize though, that the energy stored in the components as sensible heat from ambient temperature to 500°C, approximately 223.5 MJ (62.08 kWh_{th}), remains permanently stored in the TES unit as there is a defined minimum temperature limit for the heat extraction. Certainly those 62.08 kWh_{th} stored below 500°C could be used for low temperature applications such as heating water; however, the present modeling of the TES unit is not considering heat extraction below the established lower limit of 500°C.

Figure 9 shows the change in the exergy stored by the unit throughout the complete work cycle and its distribution in each of the components, calculated through Eq.4. At the last time-step of the initial charge (when the unit is fully charged) 268.4 MJ of exergy are stored, which is 59 % of the total energy stored. This value represents the maximum theoretical limit for the amount of the energy stored that could be transformed into work by an ideal engine or work producing device.

The exergy stored in the TES unit follows a very similar distribution than that of the energy, at the end of the initial charge period, 51.2% of the total exergy is stored in the glass, 19.1 % in the vertical walls, 15.3 % in the top plate and 14.4 % in the bottom plate. The stored exergy increase rate becomes smaller as the temperature of the elements rise because entropy becomes greater with increasing temperatures.

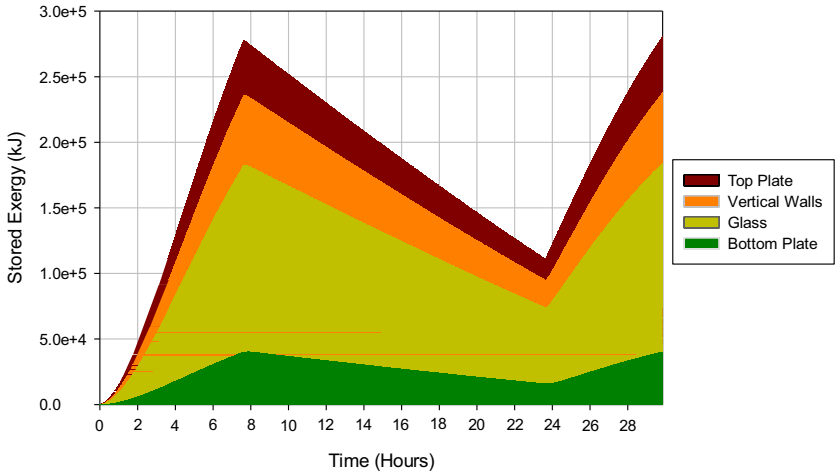

Figure 9. Exergy (work potential) stored in the TES unit throughout the complete work cycle

In order to have a proper closed cycle, the recharge period is cut before the 8 hours at the point in which the TES unit reaches its full-charge state, thus the overshoot that occurs at the end of the recharge is not considered for the round-trip exergy efficiency.

At the end of the discharge the total exergy destroyed is 0.866 MJ; which is less than 1% of the exergy stored at the beginning of the discharge. As the temperatures of the components decrease and become closer to each other the exergy destruction rate becomes smaller. Of the exergy destroyed during the discharge 50.8% occurs in the graphite walls, while the glass accounts for 26.45%, the bottom plate 22.6% and the top plate a minimal 0.14%.

During the recharge period, up to the point where the TES unit returns to the cycle initial state, the total exergy destroyed is 86.43 MJ, which represents 22.1 % of the exergy supplied by the Fresnel during that period. The amount of exergy destroyed during the discharge period is considerably smaller than during the recharge because during discharge there is only destruction due to the little heat conduction between components and the temperatures are very close to each other, while during the recharge there is a great amount of exergy input, with bigger temperature gaps and exergy is destroyed due to the actual process of storing energy.

As the temperatures of the components increase and become closer to each other the exergy destruction rate becomes smaller. Approximately 94.4% of the exergy destruction during the recharge occurs in the top plate where concentrated radiation is received, graphite walls account for 3.7 % while 1.7% is destroyed in the glass and only 0.2 % in the bottom plate.

Figure 10 presents a summary of the exergy balance of the TES unit during the discharge and recharge periods, the initial charge is not considered since it is not part of the cyclic operation, it occurs sporadically when the unit is discharged below the lower limit due to a cloudy day, for instance. Of the total 390.88 MJ (108.58 kWh_{th}) of exergy supplied by the Fresnel lens during the recharge period considered, 58.5 % is extracted from the TES for driving the Stirling engine during the discharge and recharge periods, 42.2% and 16.3% respectively, 18.7 % is lost as thermal radiation at the cavity and 22.3% is destroyed: 22.1 % during

the recharge and an almost negligible 0.22% during the discharge period.

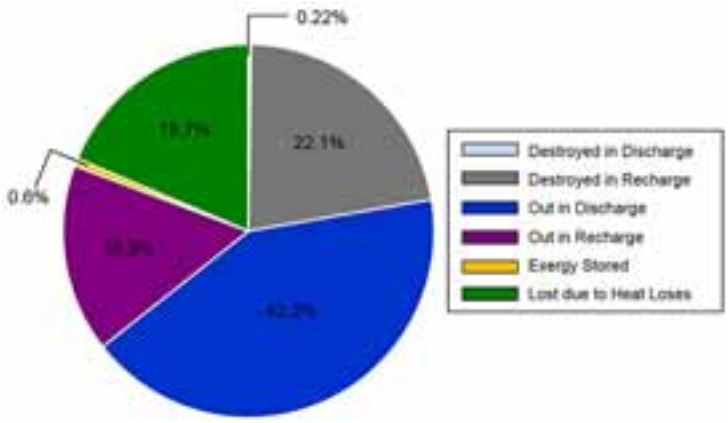

Figure 10. Exergy balance of the TES unit for the discharge and recharge periods

The TES unit has an energy-based efficiency of 72.2 % while it presents an exergy-based efficiency of 59%. In general, the energy efficiency of renewable energy systems has been found to be always greater than their exergy efficiency (Park et al. 2014), with which the analysis shown in the present paper is in agreement.

5. Shortcomings and opportunity areas in the design

This study presents a functional design for a glass-based TES unit capable of meeting the requirements of the solar driven micro-CHP system within which it will operate; nonetheless, there are still opportunity areas for the betterment of the concept, therefore optimization works should be carried out.

Preliminary tests have shown that graphite at high temperatures experiences a severe oxidation when exposed to air. The inner components are protected by contact with the molten glass; however, the issue remains for the exposed upper graphite components such as the cavity. The use of a layer of molten glass covering the interior of the receiver will be assessed, although stainless steel shields are still deemed as a good option.

The frustum-shaped receiver allows reducing radiative losses from the TES unit's inlet surface; however, its configuration has not been yet optimized. Covering the opening of the cavity with a glass plate, which is translucent to concentrated solar radiation but opaque to thermal radiation emitted by the graphite surface could help to achieve a further reduction of the radiative losses.

Although no concluding signs were found in the post-experimental assessments, devitrification of the storage medium is a latent possibility. Assuring a sufficient cooling rate for the glass in the unit is important, otherwise, it would start to devitrificate, (i.e. decompose into the elements from which it is formed). A cooling rate of approximately $8.7x10^{-3}$ Ks^{-1} is expected during the discharge of the TES unit. The critical cooling rate for silica glasses oscillates between 10^{-2} and 10^{-3} Ks^{-1} (Le Bourhis, 2008), thus the expected cooling rate of the glass in the TES unit should be sufficient for avoiding crystallization.

Theoretically, devitrification should not alter greatly the storage capacity of the TES unit. The heat capacities of silicate glasses can be closely approximated by the partial contribution of each component according to their percentage in the composition (Stebbins et al.1984, Richet, 1987), Consequently, if devitrification did occur, there would not be a significant loss in the storage capacity per unit mass of the storage medium; however, the internal thermal behavior of the TES unit could be largely modified by the different thermal conductivities of the components.

Another important area for improvement is the exergy efficiency of the storage unit. The design hereby presented attained an exergy efficiency of 59%. The internal graphite components account for a big part (~20%) of the exergy destruction. The development of a parametric model would allow improving the system in this sense by allowing exploring changes in the geometry that improve performance but don't alter much the cost of the system.

6. Concluding remarks

Soda-lime silica glass is exceedingly interesting as a sensible heat storage medium because of its elevated specific heat capacity, high chemical stability, low toxicity and flammability, and a remarkably low cost; however its use for said purpose has not been sufficiently evaluated.

A concept for a silica-glass based thermal energy storage unit for a micro-CHP system is presented. In this directly charged concept, the molten glass is enclosed in a refractory concrete container together with several narrowly spaced vertical graphite walls, whose purpose is distributing the energy uniformly throughout the storage medium. A transient mathematical model was developed for analyzing the thermal behavior of the proposed TES unit throughout the cyclic operation. The results obtained reveal a satisfactory overall performance and provide important and encouraging information. The following points may be highlighted:

- The initial charge of the unit lasts approx. 7 ⅔ hours, meaning that a unit at ambient temperature can be fully charged in 1 day time using exclusively solar power.
- Due to its effective internal design, the unit is capable of supplying the 4 kW output during the entire 16-hour discharge period maintaining a temperature superior to the 500 °C lower limit.
- During the 8-hour recharge, the unit reaches its fully charged state, whereby the continuous operation of the system is assured.

An important aspect of the mathematical modeling is the exergy analysis that was carried out. It has been found that of the total exergy (108 kWh) supplied by the solar concentrator during the recharge period, 59 % is used for driving the Stirling, 19 % is lost due to heat losses in the cavity receiver and 22 % is destroyed. The TES unit exhibits therefore an exergy efficiency of 59% while it presents an energy efficiency of 72.2%. Once the system has been further optimized, it is hoped that the combination of low-cost materials and simple fabrication could make this a cost-effective system able to meet the long term goal of $15 USD per stored kWh of heat (U.S Department of Energy, 2013).

The article presents a functional design capable of meeting the requirements of a novel solar-driven power-generation system; nonetheless, there is still a vast area of opportunity for the improvement and optimization of the proposed glass-based thermal energy storage unit.

7. Acknowledgements

The authors would like to thank the Mexican Center for Innovation in Solar Energy (CeMIE-Sol) for funding the present project through the Strategic Project #05: “Development of solar thermal storage units” and the “Energy and climate change” research group, part of the Engineering and Science School, of the Tecnológico de Monterrey for sponsoring the participation in the ISES SWC 2015.

8. References

Bapat S.G. 1973. Thermal conductivity and electrical resistivity of two types of ATJ-S graphite to 3500 K. Journal of Carbon;11: 511-514.

Bapat S.G, Nickel H. 1973. Thermal conductivity and electrical resistivity of POCO grade AXF-Q1 graphite to 3300 K. Journal of Carbon ; 11:323-327.

Butland A.T.D, Maddison R.J. 1974. The specific heat of graphite: an evaluation of measurements. Journal of Nuclear Materials ; 49: 45-56.

Cárdenas B, León N. 2013. High temperature latent heat thermal energy storage: Phase change materials, design considerations and performance enhancement techniques. Renew. Sust. Energy Rev; 27:724-737

Farid M, Khudhair A,Razack S, Al-Hallaj S. 2004. A review on phase change energy storage: materials and applications. Energy Conversion and Management; 45:1597–615

Gil A, Medrano M, Martorell I, Lazaro A, Doblado P, Zalba B, et al. 2010. State of the art on high temperature thermal energy storage for power generation. Part 1: concepts, materials and modellization.

Renew. Sust. Energy Rev; 14:31–55.

Hasnain SM. 1998. Review on sustainable thermal energy storage technologies. Part I: heat storage materials and techniques. Energy Conversion Management; 11: 1127–38.

Huang J, Gupta P.K. 1992. Temperature dependence of the isostructural heat capacity of a soda lime silicate glass. Journal of Non-Crystalline Solids; 139: 239-247.

Kenisarin M, Mahkamov K. 2007. Solar energy storage using phase change materials. Renew. Sust. Energy Rev; 11:1913–65

Le Bourhis E. Glass mechanics and technology. Wiley-VCH. Germany, 2008

Liu M, Bruno F. 2012. Review on storage materials and thermal performance enhancement techniques for high temperature phase change thermal storage systems. Renew. Sust. Energy Rev; 16:2118–32

Liu M, Gomez JC, Turchi CS, Tay NHS, Saman W, Bruno F. 2015. Determination of thermo-physical properties and stability testing of high-temperature phase-change materials for CSP applications. Solar Energy Materials & Solar Cells; 139:81–87

Madelung O, White GK. 1991. Temperature dependence of thermal conductivity of graphite. In: Thermal Conductivity of Pure Metals and Alloys, vol. 15. Springer Berlin Heidelberg. pp. 430-439

Medrano M, Gil A, Martorell I, Potau X, Cabeza L. 2010. State of the art on high- temperature thermal energy storage for power generation Part 2: case studies. Renew. Sust. Energy Rev; 14:56–72

Nihira T, Iwata T. 2003. Temperature dependence of lattice vibrations and analysis of the specific heat of graphite. Physical Review B; 68: 134305

Park S.R, Pandey A.K, Tyagi V.V, et al. 2014.Energy and exergy analysis of typical renewable energy systems. Renew. Sust. Energy Rev; 30:105-123

Petela R. 2003. Exergy on undiluted thermal radiation. Journal of Solar Energy; 74:469-88

Ramírez, Carlos. Optical design of segmented heliostat and reduced focal distance Fresnel lens for solar energy concentration. PhD thesis, ITESM, Monterrey, Mexico. 2015

Rasor NS, McClelland JD. 1960. Properties of graphite, molybdenum tantalum to their destruction temperatures. Journal of Physics and Chemistry of Solids; 15: 17-26.

Richet P. 1987.Heat capacity of silicate glasses. Journal of Chemical Geology; 62: 111-124.

Shand E.B. 1958.Glass engineering handbook. McGraw Hill.

Sharma A, Tyagi VV, Chen CR, Buddhi D. 2009. Review on thermal energy storage with phase change materials and applications. Renew. Sust. Energy Rev; 13:318–45.

Stebbins J.F, Carmichael I.S.E, Moret L.K. 1984. Heat capacities and entropies of silicate liquids and glasses. Contributions to Mineralogy and Petrology; 86:131-148.

Steinmann WD. 2015. Thermal energy storage systems for concentrating solar power technology. In: Cabeza LF (Ed.). Advances in thermal energy storage systems: Methods and applications. Woodhead Publishing, Cambridge, UK, pp.511-532.

U.S. Department of Energy, Grid energy storage. Washington, USA. 2013.

Ushak S, Fernandez AG, Grageda M. 2015. Using molten salts and other liquid sensible storage media in thermal energy storage systems. In: Cabeza LF (Ed.). Advances in thermal energy storage systems: Methods and applications. Woodhead Publishing, Cambridge, UK. pp.49-64

Wagner P, Dauelsberg LB. 1967.The thermal conductivity of ZTA graphite. Journal of Carbon, 5: 271-279.

Zalba B, Marín J, Cabeza L, Mehling H. 2003. Review on thermal energy storage with phase change: materials, heat transfer analysis and applications. Applied Thermal Engineering; 23:251–83.